

## ORIGINAL RESEARCH ARTICLE

# Type 2 diabetes-induced hyposalivation of the submandibular gland through PINK1/Parkin-mediated mitophagy

Ruo-Lan Xiang<sup>1</sup>  | Yan Huang<sup>2</sup> | Yan Zhang<sup>1</sup> | Xin Cong<sup>1</sup> | Zhe-Jing Zhang<sup>1</sup> | Li-Ling Wu<sup>1</sup> | Guang-Yan Yu<sup>2</sup>

<sup>1</sup>Center for Salivary Gland Diseases of Peking University School and Hospital of Stomatology, Key Laboratory of Molecular Cardiovascular Sciences, Ministry of Education, and Beijing Key Laboratory of Cardiovascular Receptors Research, Department of Physiology and Pathophysiology, Peking University School of Basic Medical Sciences, Beijing, China

<sup>2</sup>Department of Oral and Maxillofacial Surgery, Peking University School and Hospital of Stomatology, Beijing, China

**Correspondence**

Ruo-Lan Xiang, Key Laboratory of Molecular Cardiovascular Sciences, Ministry of Education, and Beijing Key Laboratory of Cardiovascular Receptors Research, Department of Physiology and Pathophysiology, Center for Salivary Gland Diseases of Peking University School and Hospital of Stomatology, Peking University School of Basic Medical Sciences, 100191 Beijing, China.  
Email: xiangrl@bjmu.edu.cn

**Funding information**

Beijing Natural Science Foundation, Grant/Award Number: 7162100; National Natural Science Foundation of China, Grant/Award Number: 81570993

**Abstract**

Diabetes is often accompanied by dysfunction of salivary glands. However, the molecular mechanism remains unclear. The mechanisms that underlie diabetic hyposalivation were studied by db/db mice and SMG-C6 cells. We found morphological changes and decreased stimulated salivary flow rates of the submandibular gland (SMG) in diabetic mice. We observed structural changes and dysfunction of mitochondria. More mitophagosomes and higher expression of autophagy-related proteins were detected. Increased levels of proteins PINK1 and Parkin indicate that PINK1/Parkin-mediated mitophagy was activated in diabetic SMG. Consistently, high glucose (HG) induced mitochondrial dysfunction and PINK1/Parkin-mediated mitophagy in cultivated SMG-C6 cells. HG also increased reactive oxygen species (ROS) and lessened activation of antioxidants in SMG-C6 cells. In addition, HG lowered ERK1/2 phosphorylation and HG-induced mitophagy was decreased after ERK1/2 was activated by LM22B-10. Altogether, these data suggest that ROS played a crucial role in diabetes-induced mitochondrial dysfunction and PINK1/Parkin-mediated mitophagy and ERK1/2 was required in HG-induced mitophagy in SMG.

**KEYWORDS**

hyposalivation, mitochondrion, mitophagy, submandibular gland, type 2 diabetes mellitus

## 1 | INTRODUCTION

Type 2 diabetes mellitus (T2DM) usually causes functional damage to many organ systems, such as heart, blood vessels, kidneys, and nerves system. In addition, diabetes mellitus is thought to promote hyposalivation, a qualitative and/or quantitative absence of saliva in the oral cavity (Feng et al., 2015). There are significant differences in the saliva flow between diabetic and nondiabetic patients. (Bajaj, Prasad, Gupta, & Singh, 2012). Sufficient saliva is very important to maintain oral health. Insufficient flow of saliva can lead to difficulty speaking and eating,

increased oral soft tissue ulcers, and dental caries, so the role of saliva can never be downplayed in lubrication, digestion, antimicrobial activity, calcium-phosphate homeostasis, enamel demineralization, and wound healing in the oral cavity. (Mathison, Davison, Befus, & Gingerich, 2010; Mednieks, Szczepanski, Clark, & Hand, 2009; Tickotsky & Ofran, 2017). However, there is little information on the mechanisms of salivary gland hypofunction in diabetes mellitus.

Mitochondria are essential for ensuring the energy production of cells. Convincing evidence indicates that T2DM and its complication are associated with mitochondrial structural injury and functional

This is an open access article under the terms of the Creative Commons Attribution-NonCommercial-NoDerivs License, which permits use and distribution in any medium, provided the original work is properly cited, the use is non-commercial and no modifications or adaptations are made.

© 2019 The Authors. *Journal of Cellular Physiology* Published by Wiley Periodicals, Inc.

impairment (Masser et al., 2017). Studies highlighted that high-fat diet consumption was blamed not only for peripheral insulin resistance but also heart and brain mitochondrial dysfunction and oxidative stress in rats (Pipatpiboon, Pintana, Pratchayasakul, Chattipakorn, & Chattipakorn, 2013). Studies have shown that patients with type 2 diabetes have altered mitochondrial morphology and decreased respiratory chain activity (Ritov et al., 2010). These studies suggest that mitochondria are an important player in the pathophysiology of diabetes. However, the precise role of mitochondrial dysfunction on diabetic salivary glands remains to be elucidated. The study revealed that mitochondrial dysfunction, mitochondrial membrane depolarization, and mitochondrial swelling were observed in the rat submandibular gland (SMG) 5 weeks after high-fat diet (Zalewska et al., 2013). Because mitochondria play an important role in regulating salivary secretion, the damage of mitochondrial may be related to the occurrence of salivary gland dysfunction in diabetic patients.

Mitophagy is a subtype of autophagy that selectively removes damaged mitochondria and acts as a protective mechanism to reduce oxidative stress on cells. Dysregulation of mitophagy is involved in the pathogenesis of a variety of metabolic and age-related diseases, including diabetes mellitus. In mice, a high-fat diet can lead to a decrease in mitophagy, an inflammatory response, and ultimately to impaired cellular secretion (L. Chen et al., 2017). In rat aortic endothelial cells, exogenous H<sub>2</sub>S could protect rat aortic endothelial cells from apoptosis through promoting mitophagy under high glucose and palmitate condition (Zhang et al., 2017). In addition, it has been reported that PINK1 transcription is inhibited in the skeletal muscle of type 2 diabetic patients, and the expression levels of PINK1 and Parkin proteins are reduced in the hearts of type 1 diabetic mice (Brinkmann et al., 2017). However, whether mitophagy is involved in diabetic hyposalivation and the mechanism of diabetes-inducing mitophagy in salivary gland is not well understood.

Mitochondria are a source of energy for cells, and impaired mitochondrial function may lead to organ dysfunction, including the salivary glands. Although, a role of mitochondria has been demonstrated in salivary glands function and saliva secretion, the effect of diabetes on salivary glands function, including salivary flow rate, oxidative stress, mitochondrial function, and mitophagy has never been studied. Therefore, this study is driven by the aims to explore the effect of diabetes on salivary glands function.

## 2 | MATERIAL AND METHODS

### 2.1 | Laboratory animals

Male leptin receptor-deficient db/db mice aged 16 weeks (a model of spontaneous T2 DM) ( $n = 6$ ) and db/m mice ( $n = 6$ ) were supplied by ChangZhou Cavens Laboratory Animal Ltd. All experimental procedures were approved by the Animal Research Ethics Committee of Peking University Health Science Center, and were in accordance with the *Guidelines for the Care and Use of Laboratory Animals* (NIH Publication No. 85-23; revised 1996). The blood glucose levels were determined from tail venous blood using Glucometer (ACCU-CHEK

and iodine [125I]-Insulin Radioimmunoassay Kit (Union Medical & Pharmaceutical Technology Ltd) to determine blood glucose and serum insulin levels, respectively.

### 2.2 | Cell culture

The culture of the rat SMG cell line SMG-C6 cells was carried out in the method described previously (Xiang, et al., 2014). SMG-C6 cells were incubated for 24 hr in medium containing high glucose (25 mM) and mannitol was used as an osmotic pressure control (25 mM).

### 2.3 | Histological stain

SMG, parotid, and sublingual glands were stained with hematoxylin and eosin staining (H&E), respectively. Under an optical microscope (Q550CW; Leica) SMG granular ductal kinin was stained with p-dimethylaminobenzaldehyde (DMAB) staining. The morphological changes were obtained.

### 2.4 | Measurement of SMG stimulated saliva flow

After anesthesia, chloral hydrate (0.4 g/kg body weight) was intraperitoneally injected, the SMG duct was separated and a capillary tube was inserted. Stimulated saliva volume was measured 10 min after intraperitoneal injection of pilocarpine (10  $\mu$ g/g body weight).

### 2.5 | Transmission electron microscopy

Small pieces of mouse SMG tissues were fixed with 5% glutaraldehyde. SMG-C6 cells were washed and fixed with 2% glutaraldehyde. Ultrathin sections were examined with a transmission electron microscope (H-7000; HITACHI).

### 2.6 | Western blot analysis

Protein extraction of SMG tissues and SMG-C6 cells and western blot analysis were performed as previously described (Xiang et al., 2014). The antibodies used were as follows: microtubule-associated protein1 light chain 3 (LC3), Beclin-1, SQSTM1/p62, peroxisome proliferator-activated receptor  $\gamma$  coactivator-1 $\alpha$  (PGC-1 $\alpha$ ), nuclear respiratory factor-1 (NRF-1), PTEN induced putative kinase 1 (PINK1), Parkin, extracellular regulated protein kinases1/2 (ERK1/2), phospho-ERK1/2, c-Jun NH2-terminal kinase (JNK), phospho-JNK, p38, phospho-p38 (all 1:1,000; Cell Signal Technology), and  $\beta$ -actin (1:4,000; Abcam)

### 2.7 | ATP measurements

According to the program provided by the manufacturer, ATP content in SMG tissues and SMG-C6 cells was measured using the ATP-Lite detection Kit (Vigorous Biotechnology) based on the luciferase reaction with luciferin as well as the photometer. All experiments were repeated three times, and protein concentration was determined before all ATP content detection (Zhang et al., 2017).

## 2.8 | Determination of mitochondrial DNA copy number

Genomic DNA was isolated using a genomic DNA kit (Zoman Biotech). The q-PCR method was used to reflect the copy number of mitochondrial DNA (mtDNA) by the ratio of the number of Cyt B to the number of  $\beta$ -actin in the genome (Venegas & Halberg, 2012).

## 2.9 | Reactive oxygen species detection

The levels of mitochondrial reactive oxygen species (ROS) generation were determined by using 10  $\mu$ M 2,7-dichlorofluorescein diacetate (DCFH-DA; Sigma-Aldrich) for 30 min at 37°C, and then the fluorescence intensity was measured using a fluorescent microplate reader (EnSpire Multimode Plate Reader, Perkin Elmer, Waltham, MA).

## 2.10 | Measurement of mitochondrial membrane potential

The mitochondrial membrane potential ( $\Delta\Psi_m$ ) change was determined by incubating with 5  $\mu$ M JC-1 (5,5',6,6'-tetrachloro-1,1',3,3'-tetraethylbenzimidazol-carbocyanine iodide) staining at 37°C for 30 min, and then the fluorescence intensity was obtained using a fluorescent microplate reader (EnSpire Multimode Plate Reader). The mitochondrial membrane potential was detected by the ratio of red-green fluorescence intensity of the cells by in JC-1 staining.

## 2.11 | Detection of oxidative stress

Glutathione (GSH), superoxide dismutase (SOD), and glutathione peroxidase (GPX) are important antioxidants that scavenge free radicals. The GSH concentration was measured using a kit (Beyotime Institute of Biotechnology) according to the manufacturer's instructions.

## 2.12 | Oxygen consumption rate measurements

Mitochondrial respiration of SMG-C6 cells was performed using an XF24 Extracellular Flux Analyzer (Seahorse Biosciences). Oxygen consumption rate (OCR) was assessed in living cells that were analyzed at baseline and following the sequential addition of culture medium, oligomycin, and mitochondrial inner membrane uncoupler (FCCP), according to the manufacturer's protocol.

## 2.13 | Detection of cell activity

Cell activity was assessed by means of the 3-(4,5-dimethylthiazol-2-yl)-2,5-diphenyl tetrazolium bromide (MTT) assay. The MTT assay was applied to determine cell viability using a 96-well plate reader (EnSpire Multimode Plate Reader).

## 2.14 | Immunofluorescence staining

Mitochondria stained with MitoTracker Green and lysosome stained with LysoTracker Red (Invitrogen). Mitochondria and lysosomes were

traced in live cells by incubation with MitoTracker Green (200 nM) and LysoTracker Red (50 nM), respectively, at 37°C for 10 min. Fluorescence images were taken by confocal microscopy (TCS SP8; Leica).

## 2.15 | Knockdown of Parkin

The siRNA of Parkin was produced by Origene Technologies (Origene). SMG-C6 cells were transfected with siRNA by Lipofectamine 2000 (Invitrogen) according to the manufacturer's instructions.

## 2.16 | Statistic analysis

Two groups of t-test and one-way analysis of variance were used for statistic analysis, and multiple groups of Bonferroni's test were used as appropriate. Means  $\pm$  standard error of mean were used to represent the data. All tests were of bilateral significance, \* $p < .05$ ; \*\* $p < .01$ . All statistics were completed using GraphPad Prism 5.0 software.

# 3 | RESULTS

## 3.1 | General characterization of salivary glands in diabetic mice

The mean random serum glucose level of db/db mice was about 2.6 times greater than that of db/m mice, and their mean serum insulin level was about 1.7 times greater than that of control mice (Figure 1a,b). Next, we study the basic changes of salivary glands in db/db mice. Compared with the control group, the body weight and body size of the db/db mice were remarkably larger than the db/m mice, but the weight and size of the SMG and parotid glands of the db/db mice were significantly lower than those of the control mice (Figure 1d). However, the weight and size of sublingual gland do not differ between db/db and db/m groups (Figure 1c,g). These results indicated that the influence on the weight and size of SMG and parotid gland were observed in db/db mice.

## 3.2 | Diabetic SMG is impaired in the morphology and secretion

H&E staining suggested marked acinar enlargement and ductal atrophy in db/db mice (Figure 2a-e). Dimethylaminobenzaldehyde staining further confirmed a decrease in the number of granular convoluted tubes in diabetic SMG (Figure 2f,g). Oil Red O staining also suggested no fat deposition in diabetic SMG (Figure 2h). Nevertheless, these pathology changes of H&E images were not observed in the parotid gland and sublingual gland (Figure 2i,j). These results indicate that diabetes mellitus selectively leads to characteristic histological changes of SMG in db/db mice.

We further studied the effect of diabetes mellitus on the secretory function of SMG. Blood flow takes part in the formation of saliva. Blood flow in SMG of db/db mice was significantly reduced by approximately 13.6% (Figure 2k). Moreover, the salivary flow rate in diabetic SMG was significantly decreased by 67.2% after pilocarpine

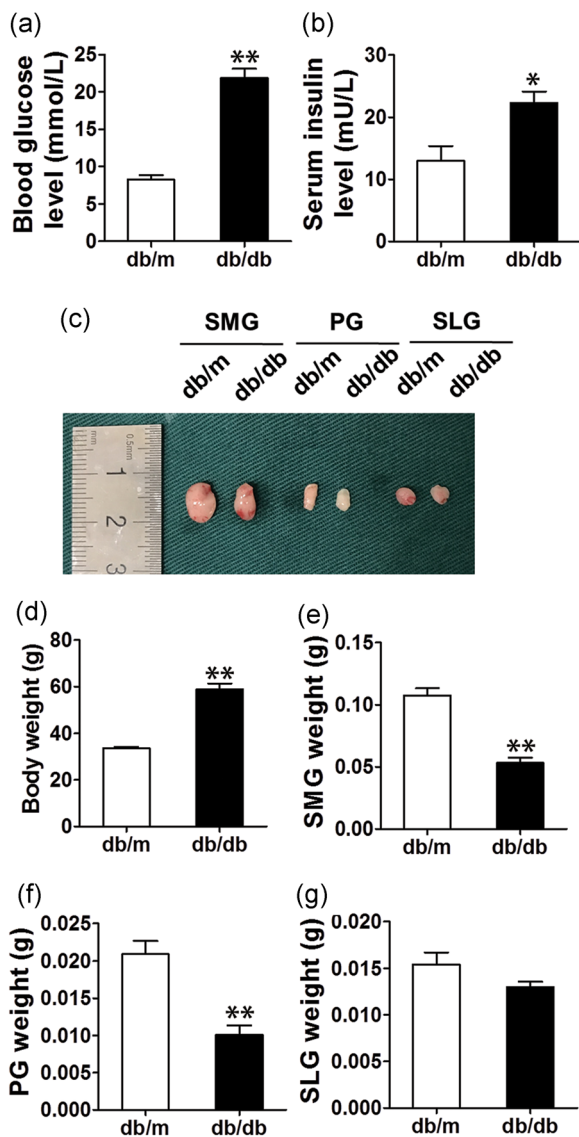


**FIGURE 1** General characterization of salivary glands in diabetic mice. (a, b) The levels of blood glucose and serum insulin. (c) The pictures of SMG, PG, and SLG in db/m and db/db mice. (d) The body weight of db/m and db/db mice. (e–g) The weights of SMG, PG, and SLG.  $n = 5-6$ ,  $*p < .05$  and  $**p < .01$ . PG, parotid gland; SLG, sublingual gland; SMG, submandibular gland

stimulation 10 min (Figure 2). These *in vivo* results suggested that diabetes mellitus reduces the secretion of SMG in db/db mice.

### 3.3 | Diabetes mellitus induces mitochondrial dysfunction in diabetic SMG

Saliva secretion critically depends on mitochondrial respiratory capacity and appropriate ATP concentration. In the db/db group, approximately 46.54% of the mitochondria showed cristae disorders, and increased mitochondrial volume was observed under the transmission electron microscope (Figure 3a–c). The mtDNA copy number was significantly reduced to 34.7% in diabetic SMG

compared with those in db/m mice (Figure 3d). Furthermore, JC-1 staining and the measurement of ATP content were used to detect mitochondria function. Here, we found that the mitochondrial membrane potential was decreased by 52.6% and ATP content was also decreased by 50% in diabetic SMG. Altogether, these data support that mitochondrial dysfunction was induced by diabetes mellitus in SMG of db/db mice.

In addition, we measured the protein expression of mitochondrial biogenesis marker, PGC-1 $\alpha$ , and NRF-1, which plays a critical role in the regulation of mitochondrial biogenesis. We found that protein expressions of PGC-1 $\alpha$  and NRF-1 between db/m and db/db mice (Figure 3g–i) are not changed, and therefore the mitochondrial dysfunction in diabetic SMG is not related to mitochondrial biogenesis.

### 3.4 | Diabetes induces PINK1/Parkin-mediated mitophagy in diabetic mice

Mitophagy can eliminate aging and damage to mitochondrial, which is important for control of mitochondrial quality (Nacarelli, Azar, & Sell, 2016). We first analyzed the expression of proteins involved in autophagic processes. LC3II is the marker for autophagosome formation, whereas p62 is the marker of autophagolysosome degradation. First, we found a significant increase in LC3-II and Beclin-1 in db/db mice SMG, whereas the expression of p62 was significantly downregulated compared with the db/m group (Figure 4a–d). A transmission electron microscope was exploited for a further direct evidence of mitophagy. Figure 4e showed that the number of typical mitophagy was significantly increased in the db/db group compared to the db/m one, characterized by double-membraned vacuoles that phagocytize mitochondrially. The PINK1/Parkin-mediated pathway is one of the most mature mitophagy pathways in mammals (Jin et al., 2018). We found that in db/db mice, PINK1 protein levels increased by 109% and Parkin protein levels increased by 116% (Figure 4f–h). These results suggested that PINK1/Parkin-mediated mitophagy was activated in diabetic SMG.

### 3.5 | High glucose-induced mitochondrial dysfunction and PINK1/Parkin-mediated mitophagy in SMG-C6 cells

To determine whether high glucose (HG) induced mitochondrial dysfunction and mitophagy, we used 25 mM glucose to stimulate SMG-C6 cells 24 hrs. Consistent with previous findings, mtDNA copy number, mitochondrial membrane potential, and ATP content were significantly decreased under HG conditions compared with the normal glucose control group (Figure 5a–c). Next, the method of oxygen consumption rate (OCR) was used to observe mitochondrial respiratory function. In HG-treated SMG-C6 cells, a significant decrease in the maximal OCR and spare OCR was observed compared with the normal glucose group (Figure 5e–i). These results suggest that HG induces the mitochondrial dysfunction in SMG-C6 cells.

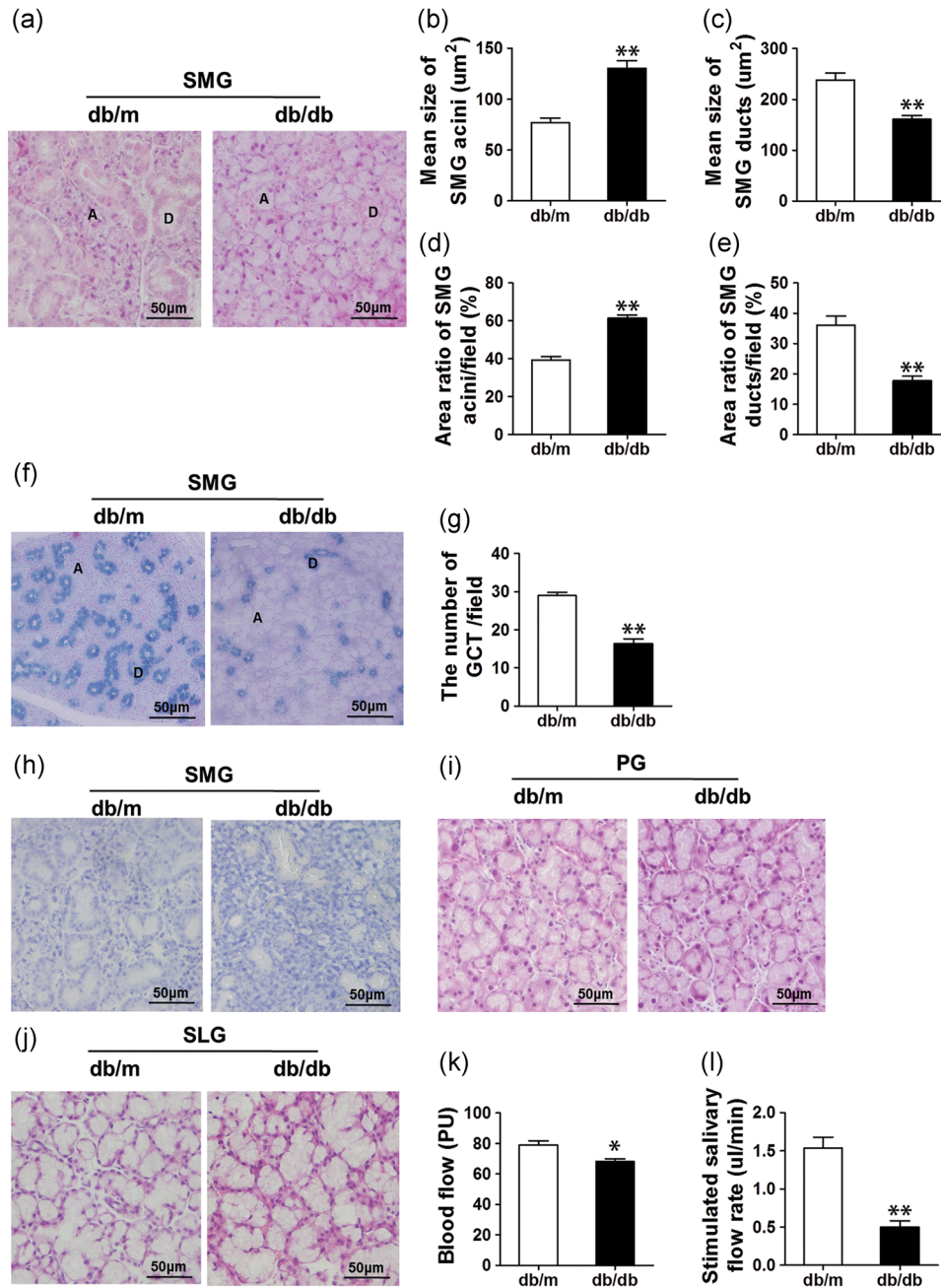


**FIGURE 2** Morphology and secretion of SMG are impaired in diabetic mice. (a) H&E staining of SMG from db/m and db/db mice. Scale bars, 50 μm. (b,c) Mean size of acini and ducts. (d,e) Mean area ratio of acini and ducts in each field of view. (f) DMAB staining of SMG from db/m and db/db mice. Scale bars, 50 μm. (g) The mean number of granular convoluted tubules in each field of view. (h) Oil Red O staining of SMG. Scale bars, 50 μm. (i,j) H&E staining of PG and SLG. Scale bars, 50 μm. (k) SMG blood flow was measured by using laser-Doppler stainless steel probe. (l) Salivary flow rates (μl/min) of SMG were measured after pilocarpine stimulation 10 min.  $n = 5-6$ ; \* $p < .05$ ; \*\* $p < .01$ . DMAB, dimethylaminobenzaldehyde; H & E, hematoxylin and eosin; PG, parotid gland; SLG, sublingual gland; SMG, submandibular gland

We also examined whether the mitochondrial dysfunction in SMG-C6 cells caused by cell damage or osmolarity. Here, we found that no change in cell viability is likely due to the HG treatment (Figure 5d). SMG-C6 cells grown in normal medium supplemented with 25 mM mannitol (as an osmotic control) showed no change in ATP content (Figure 5c). These analyses demonstrated that cell damage and osmolarity did not induce mitochondrial dysfunction in SMG-C6 cells.

Then we observed the mitophagy level on SMG-C6 cells increased levels of LC3-II, PINK1, and Parkin in the HG group strongly suggest enhanced mitophagy (Figure 6a-d). SMG-C6 cells grown in normal medium supplemented with 25 mM mannitol showed no change in LC3-II, PINK1, and Parkin protein levels compared with untreated cells. These analyses demonstrated that osmolarity did not stimulate mitophagy in SMG-C6 cells (Figure 6a-d). Moreover, we found that the number of mitophagosomes was highly increased under HG condition under a

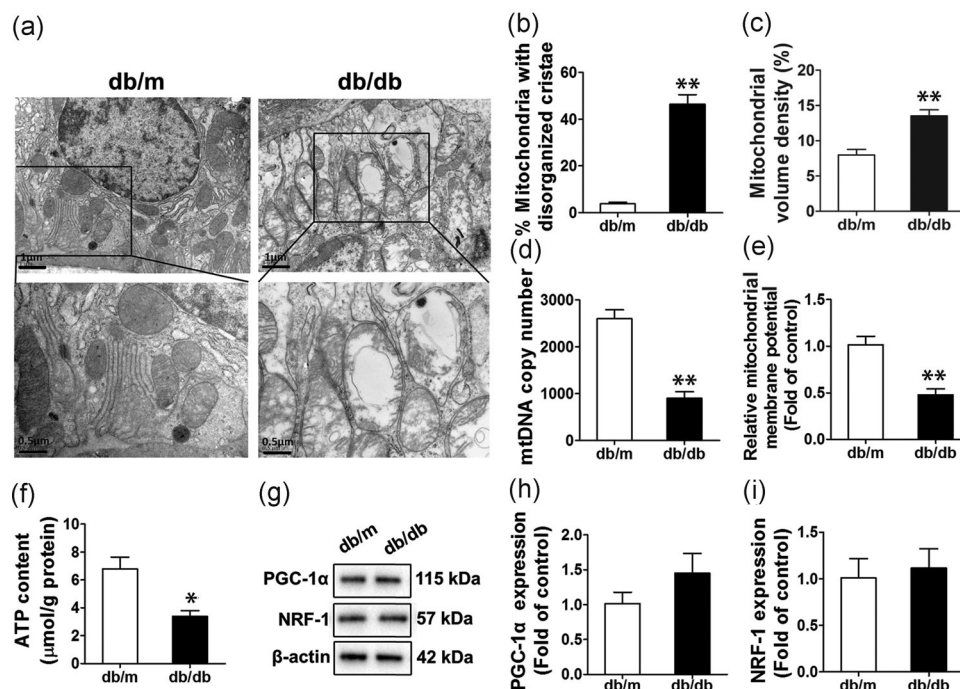


**FIGURE 3** Diabetes mellitus induced mitochondrial dysfunction in diabetic SMG. (a) Representative transmission electron microscopy images of SMG from db/m and db/db mice. Scale bars: 0.5 and 1  $\mu\text{m}$ , respectively. Quantitative analyses of mitochondrial volume density (b) and cristae morphology (c) in db/m and db/db mice. Quantitative analysis of mtDNA copy number (d), mitochondrial membrane potential (e) and ATP content (f) in db/m and db/db mice. (g–i) Expressions of PGC-1 $\alpha$  and NRF-1 were detected by western blot analysis.  $n = 5–6$ ; \* $p < .05$ ; \*\* $p < .01$ . mtDNA, mitochondrial DNA; NRF-1, nuclear respiratory factor-1; PGC-1 $\alpha$ , peroxisome proliferator-activated receptor  $\gamma$  coactivator-1 $\alpha$ ; SMG, submandibular gland

transmission electron microscope (Figure 6e). Immunofluorescence image shows a higher colocalization of lysosome with mitochondria in SMG-C6 cells that under HG condition (Figure 6f). Evidence for mitochondrial fusion with lysosomes strongly suggests that mitophagy selectively degrades mitochondria under HG stimulation, a phenomenon that is manifested by a significant increase in yellow spots. In addition autophagy in SMG-C6 cells was inhibited by 3-methyladenin (3-MA). We found that the HG-induced a decrease in ATP content (Figure 6g). These data suggested that increased mitophagy contributes to removes damaged mitochondria as a cytoprotective mechanism. Then, SMG-C6 cells were transfected with Parkin-specific siRNA or scrambled control (Figure 6h,i). HG-induced increase of LC3-II and Beclin-1 were markedly inhibited (Figure. 6j–l). Taken together, these findings indicate HG induces the PINK1/Parkin-mediated mitophagy in SMG-C6 cells.

### 3.6 | Increased ROS is responsible for mitochondria dysfunction and mitophagy in SMG-C6 cells

Next, we explored what factors were involved in the occurrence of mitophagy. It has been suggested that mitophagy initiation requires ROS signaling. HG treatment was found to increase significantly the levels of ROS in SMG-C6 cells (Figure 7a). Meanwhile, biomarkers of oxidative stress including cellular GSH, SOD, and GPX were detected. The excessive ROS production resulted in a significant reduction in levels of antioxidant factors, such as GSH, SOD, and GPX and an imbalance of the redox status (Figure 7b–d).

To determine whether ROS generation plays a role in the HG-induced mitochondria dysfunction and mitophagy, SMG-C6 cells were pretreated with ROS scavenger N-acetylcysteine (NAC, 50  $\mu\text{M}$ ) for 1 hr. Compared with control cells, pretreatment with NAC significantly blocked HG-induced ATP level depletion (Figure 7e). Seahorse metabolic flux analyzer showed that NAC pretreatment significantly recovered the maximal and spare OCR to 156.1% and 172.4%, respectively (Figure 7f–j).

Additionally, NAC preincubation remarkably inhibited HG-induced upregulation of LC3-II and Parkin (Figure 7k–m). The phenomenon of colocalization of lysosome and mitochondria in NAC-pretreated cells was significantly inhibited compared to the control group (Figure 7n). Altogether, these findings provide direct evidence of diabetes-induced mitochondria dysfunction and mitophagy associated with increased ROS.

### 3.7 | ERK1/2 is required for HG-induced mitophagy

In the end, the possible molecular mechanisms that regulate mitophagy was expected to be identified. MAPK family seems to take a key role in regulating Parkin expression. Figure 8a and b exhibit that HG treatment lessened the level of p-ERK1/2 as compared to the control group. However, the levels of p-JNK and p-p38 MAPK remained unchanged (Figure 8c–f). ERK1/2, p38MAPK, and JNK did not differ in total amount after HG treatment in 24 hr. ERK1/2 seems to be selectively regulated by HG in SMG-C6 cells rather than p38 MAPK or JNK.

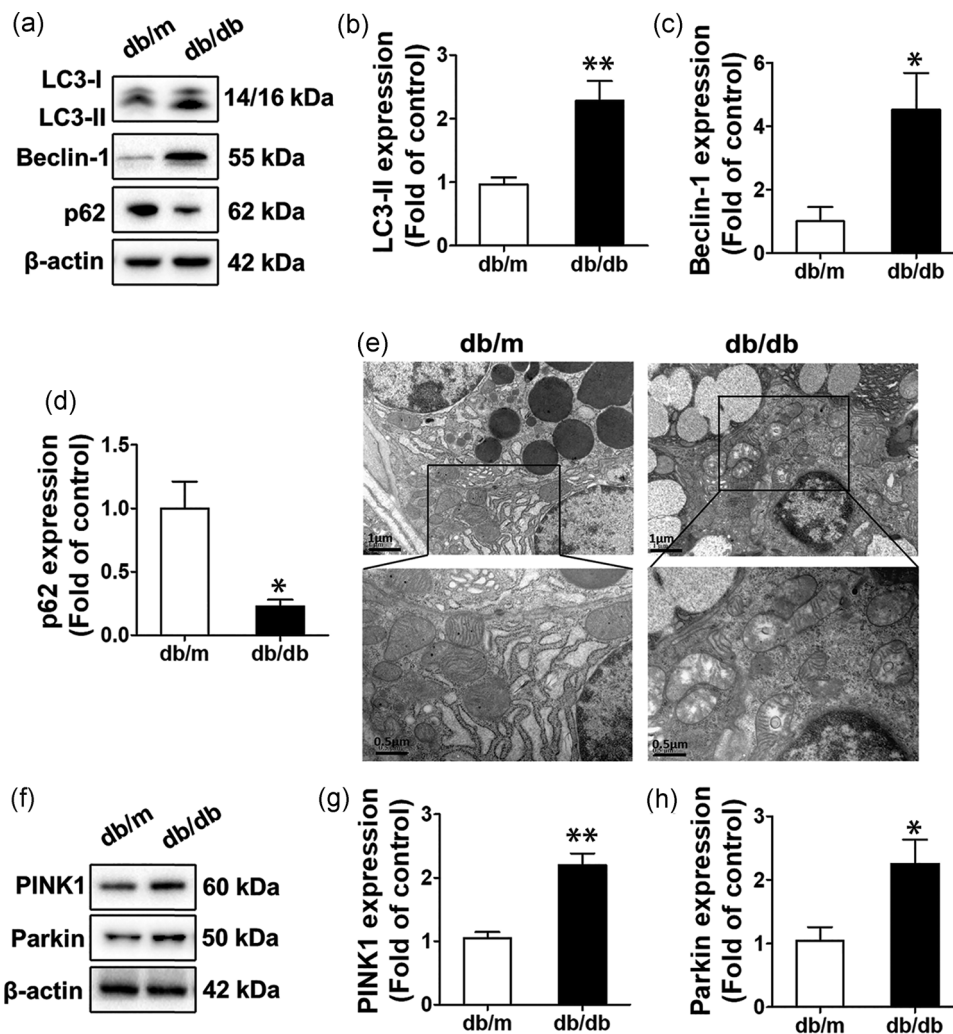


**FIGURE 4** PINK1/Parkin-mediated mitophagy is activated in diabetic SMG. (a–d) Expressions of LC3, Beclin-1, and p62 of SMG were detected by western blot analysis in db/m and db/db mice. (e) Transmission electron microscopy images of SMG from db/m and db/db mice. Scale bars: 0.5 and 1  $\mu$ m respectively. (f–h) Western blot analysis of PINK1 and Parkin of SMG in db/m and db/db mice.  $n = 5$ – $6$ ; \* $p < .05$ ; \*\* $p < .01$ . LC3, microtubule-associated protein1 lightchain 3; PINK1, PTEN induced putative kinase 1; SMG, submandibular gland

To explore whether ERK1/2 mediates the induction of mitophagy by HG, SMG-C6 cells were processed in 30 min by using 1  $\mu$ M LM22B-10 (an ERK1/2 activator) and then incubated with HG for 24 hr (Figure 8g,h). After activation of ERK1/2 under HG treatment, mitophagy was reduced, and LC3-II and Parkin expression were decreased (Figure 8i–k). These data demonstrated that HG-induced mitophagy is blocked. The results suggested that ERK1/2 plays a key role in diabetes-induced mitophagy.

## 4 | DISCUSSION

In this study, we demonstrate that diabetes mellitus reduces the salivary secretion of SMG in db/db mice. SMG in db/db mice and HG-treated cultured SMG-C6 cells showed significant mitochondrial dysfunction and activated PINK1/Parkin-mediated mitophagy. Increased mitophagy contribute to eliminating damaged mitochondria. We revealed that increasing of ROS production plays a vital role in

diabetes-induced mitochondrial dysfunction and mitophagy. Furthermore, ERK1/2 was responsible for HG-induced mitophagy. This study should provide novel insights into the mechanism by which diabetes induce hyposalivation.

T2DM can cause a number of systemic complications, including morphological and functional changes in the salivary glands (Malicka, Kaczmarek, & Skoskiewicz-Malinowska, 2015). Morphological changes in the salivary glands of diabetic patients, including changes in the density of secretory granules, lead to salivary gland diseases that affect oral health. (Lilliu et al., 2015; Lima et al., 2017; Mednieks et al., 2009). In our study, we found that diabetes leads to characteristic histological changes and reduced secretion of SMG in db/db mice. Nevertheless, these pathology changes were not available in the parotid and sublingual gland. These observations demonstrated that diabetes-induced changes of the salivary glands predominantly occurred in SMG, not in the parotid gland and sublingual gland in db/db mice.

Mitochondria is a key player in maintaining cellular metabolic homeostasis. Previous studies have demonstrated that the progress

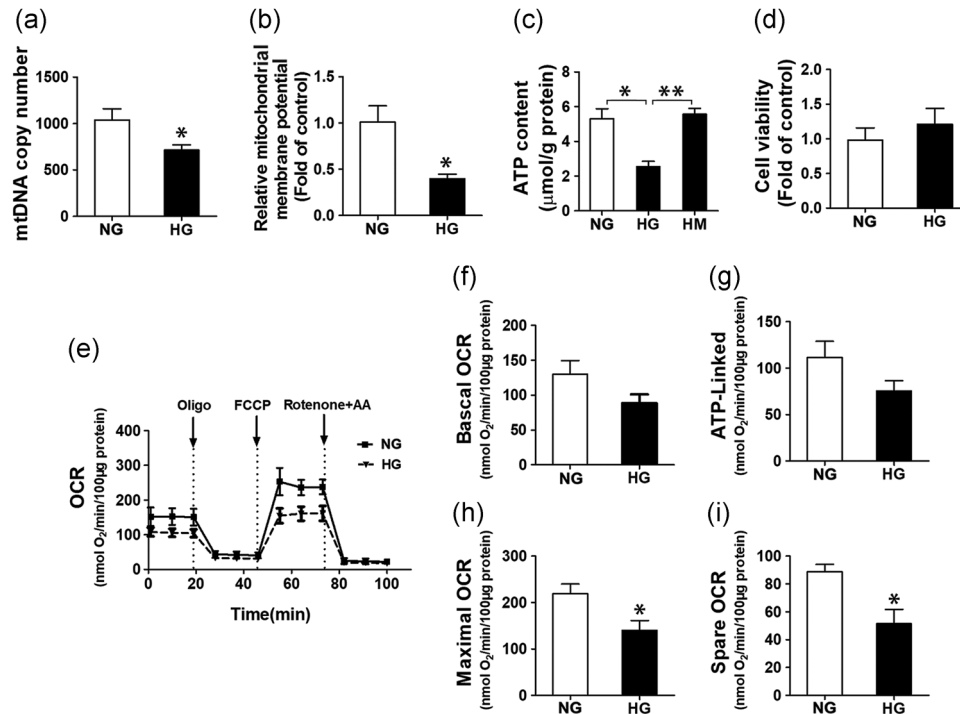


**FIGURE 5** HG induces mitochondrial dysfunction in SMG-C6 cells. Quantitative analysis of mtDNA copy number (a), mitochondrial membrane potential (b) and ATP content (c) in SMG-C6 cells after HG treatment. (d) The effects of HG on the viability of SMG-C6 cells. Representative graph (e) and quantitative analyses of basal (f), ATP-Linked (g), maximal (h), and spare (i) OCR in SMG-C6 cells after HG treatment. *n* = 3; \**p* < .05; \*\**p* < .01. HG, high glucose; HM, mannitol; mtDNA, mitochondrial DNA; NG, normal glucose; OCR, oxygen consumption rate; SMG, submandibular gland

of diabetes mellitus may be related to mitochondrial dysfunction (Bhatti, Bhatti, & Reddy, 2017; Blake & Trounce, 2014; Larsen et al., 2011). Mitochondria in type 2 diabetic patients are smaller than those in healthy people. Hyperglycemia can cause mitochondrial disruption and reduce mitochondrial content in different cell types, including heart, liver, skeletal muscle, cardiovascular, or pancreas (Jitrapakdee, Wutthisathapornchai, Wallace, & MacDonald, 2010; Kelley, He, Menshikova, & Ritov, 2002; Morino et al., 2012; Yu, Robotham, & Yoon, 2006). Although mitochondria have key roles in many cell types, there are few data regarding its role in the diabetic hyposalivation of salivary glands. Saliva secretion critically depends on mitochondrial respiratory capacity and appropriate ATP concentration. Recent studies have shown that mitochondria plays an important role in regulating the Ca<sup>2+</sup> mobilization pathway in human SMG cells (Ittichaicharoen et al., 2017). Therefore, mitochondrial damage often leads to impaired SMG function. Here, we confirmed that mitochondria showed significant histological changes and dysfunction in db/db mice and HG treated SMG-C6 cells. The results suggested that SMG in db/db mice and HG-treated cultured SMG-C6 cells showed significant mitochondrial dysfunction.

Mitophagy selectively degrades damaged mitochondria and plays a key role in maintaining mitochondrial quality (Shi, Guberman, & Kirshenbaum, 2017). Mitophagy was involved in the pathology of diabetes mellitus and its complications (Baltrusch, 2016; Cong et al.,

2017). In autophagy-deficient mice, restoring mitophagy may alleviate the myocardial damage caused by diabetes. This phenomenon favors the notion that Parkin-mediated mitophagy has a protective effect on pancreatic β-cell function in diabetes (Hoshino et al., 2014). However, excessive induction of mitophagy may destroy the mitochondria and lead to cell death and dysfunction. HG can induce mitochondrial dysfunction and mitophagy in retinal Müller glial cells, and these changes lead to a decrease in the number of mitochondria. (Devi, Somayajulu, Kowluru, & Singh, 2017). These reports indicated that only dysregulated mitophagy is detrimental. However, the functional role of mitophagy in diabetic SMG and the specific regulatory mechanism remain to be determined. Here, we confirmed that PINK1/Parkin-mediated mitophagy was significantly increased in db/db mice and HG treated SMG-C6 cells. We believed that severe stress (or damage) to mitochondria occurs during the diabetic episode and activated mitophagy can eliminate the damaged mitochondria and help maintain a healthy mitochondrial number.

We also investigated the possible mechanisms governing mitophagy in SMG. Convincing evidence indicates that ROS are now recognized as important activators of mitophagy (Sindhu et al., 2018; Vernon & Tang, 2013; Volpe, Villar-Delfino, Dos Anjos, & Nogueira-Machado, 2018). Parkin recruitment to mitochondria triggers mitophagy, and ROS is a key factor in the activation process. In addition, the p38 signaling pathway is also involved in ROS-induced mitophagy

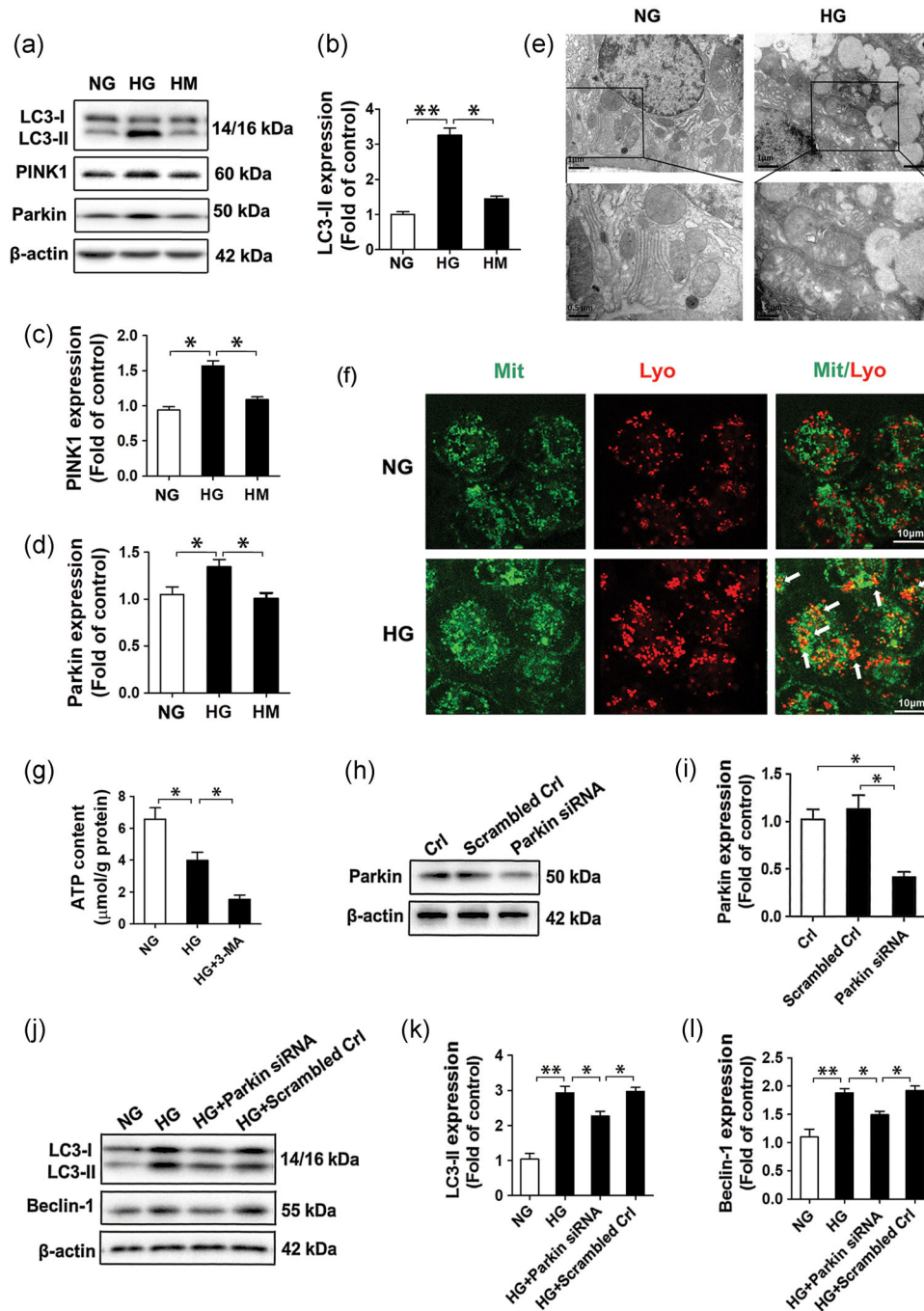


**FIGURE 6** HG induces PINK1/Parkin-mediated mitophagy in SMG-C6 cells. (a–d) Expressions of LC3, PINK1 and Parkin proteins were detected by western blot analysis after HG treatment.  $n = 6$ ;  $*p < .05$ ;  $**p < .01$ . (e) Transmission electron microscopy images in SMG-C6 cells. Scale bars: 0.5 and 1  $\mu\text{m}$ , respectively.  $n = 3$ . (f) Double immunofluorescent assay for mitochondria (green dots) and lysosome (red dots) in SMG-C6 cells.  $n = 6$ . (g) SMG-C6 cells were pretreatment with 3-MA. ATP content was measured after HG treatment.  $n = 6$ ;  $*p < .05$ ;  $**p < .01$ . (h, i) Western blot identification of Parkin in SMG-C6 cells transfected with Parkin siRNA.  $n = 3$ ,  $*p < .05$ . (j–l) Expressions of LC3 and Beclin-1 in SMG-C6 cells transfected with Parkin siRNA.  $n = 6$ ,  $*p < .05$  and  $**p < .01$ . HG, high glucose; LC3, microtubule-associated protein1 lightchain 3; Lyo, lysosome; Mit, mitochondria; NAC, N-acetylcysteine; NG, normal glucose; PINK1, PTEN induced putative kinase 1; SMG, submandibular gland; 3-MA, 3-methyladenin

(Xiao et al., 2017). Our results suggest that diabetes not only directly induces ROS production but also reduces the ability of the cells to scavenge oxygen free radicals, both of which exacerbate ROS-mediated oxidative damage. These findings presented direct

proof to mitochondria dysfunction induced by diabetes mellitus and association of PINK1/Parkin-mediated mitophagy with increased ROS.

We next explored the signaling pathway linking diabetes to mitophagy. Recent studies indicate that a few MAPK family

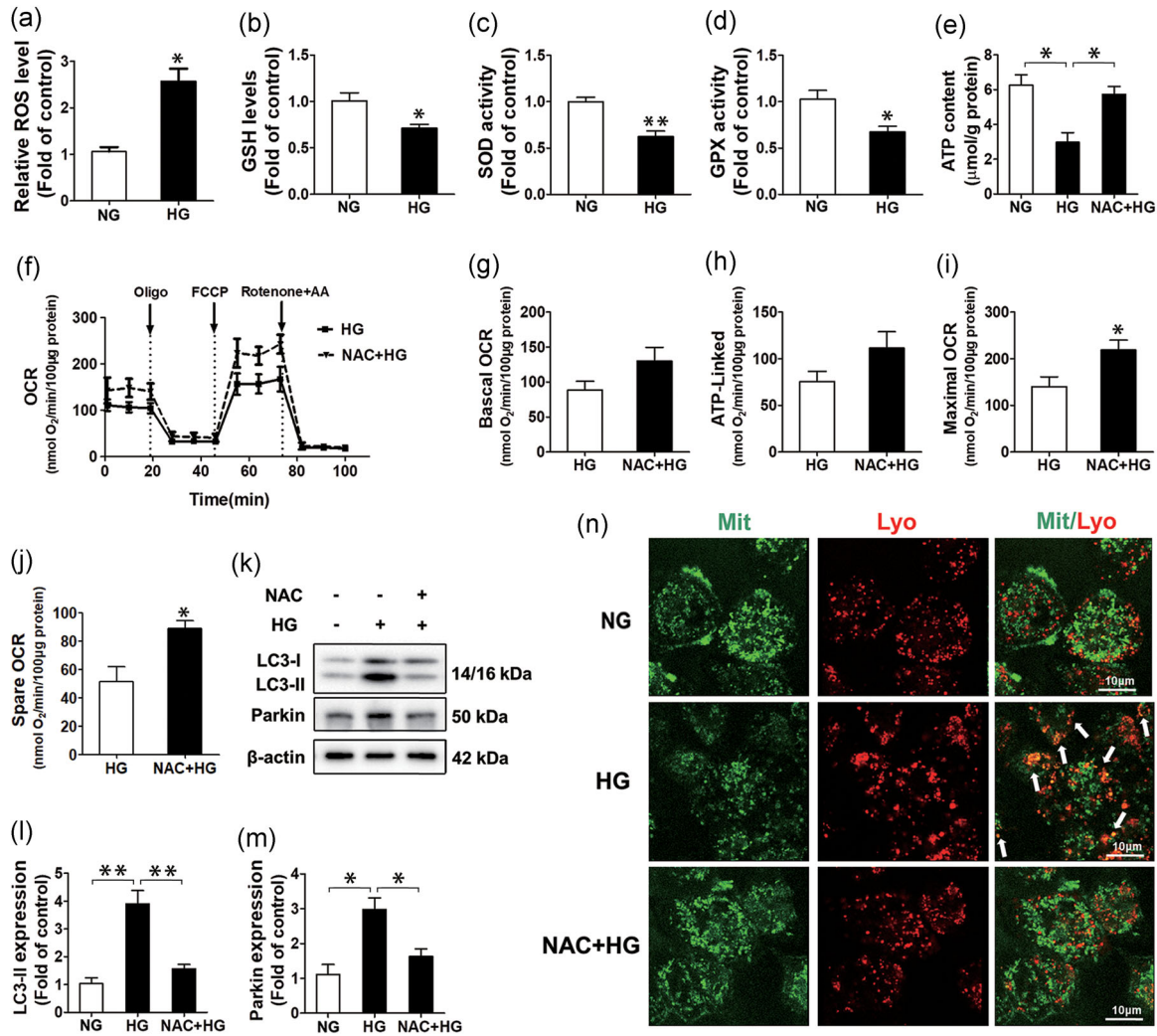


**FIGURE 7** Increased ROS is required to mediate HG-induced mitochondria dysfunction and mitophagy in SMG-C6 cells. (a) Quantitative analysis of ROS production in SMG-C6 cells after HG treatment. Quantitative analysis the levels of antioxidant factors, such as GSH (b), SOD (c), and GPX (d), respectively. SMG-C6 cells were pretreated with NAC 50  $\mu\text{M}$  for 1 hr.  $n = 3$ ;  $*p < .05$ ;  $**p < .01$ . ATP content (e) was measured.  $n = 6$ ;  $*p < .05$ . Representative graph (f) and quantitative analyses of basal (g), ATP-Linked (h), maximal (i), and spare (j) OCR after NAC pretreatment. (k-m) Expressions of LC3 and Parkin were detected by western blot analysis.  $n = 3$ ;  $*p < .05$ . (o) Double immunofluorescent assay for mitochondria (green dots) and lysosome (red dots) in SMG-C6 cells.  $n = 6$ . GSH, glutathione; GPX, glutathione peroxidase; HG, high glucose; LC3, microtubule-associated protein1 lightchain 3; Lyo, lysosome; Mit, mitochondria; NAC, N-acetylcysteine; NG, normal glucose; ROS, reactive oxygen species; SOD, superoxide dismutase; SMG, submandibular gland

members are involved in the modulation of mitophagy. ROS activates JNK and ERK1/2 MAPK signaling pathways significantly increases the stability of PINK1 and the interaction between PINK1 and Parkin (Park et al., 2017). However, F. Chen et al. (2019) found that zearalenone significantly activated autophagy by inhibited the mTOR and ERK1/2 signaling pathways in mouse ovarian granulosa cells. These reports suggest that the mechanism of activating autophagy and mitophagy might be dependent on different cell types. In the present study, we found that SMG-C6 cells exhibited a significant decrease in p-ERK1/2 levels after HG treatment and insignificant reduction of p-p38MAPK/p-JNK levels. Activation of ERK1/2 by pharmacological activator

suppressed the diabetes-induced mitophagy, indicating that ERK1/2 was the signal transduction molecule that regulates mitophagy in diabetic mitochondria in SMG-C6 cells.

In summary, we demonstrated that diabetes leads to a characteristic hyposalivation of SMG in db/db mice, which is accompanied by increased mitochondrial dysfunction and PINK1/Parkin-mediated mitophagy. The increased ROS production may be responsible for modulating mitophagy in diabetic SMG. Furthermore, ERK1/2 was required for diabetes-induced mitophagy. This study gives us novel insights into the mechanism by which diabetes causes hyposalivation and improved our understanding of decreased SMG secretion of in diabetes.

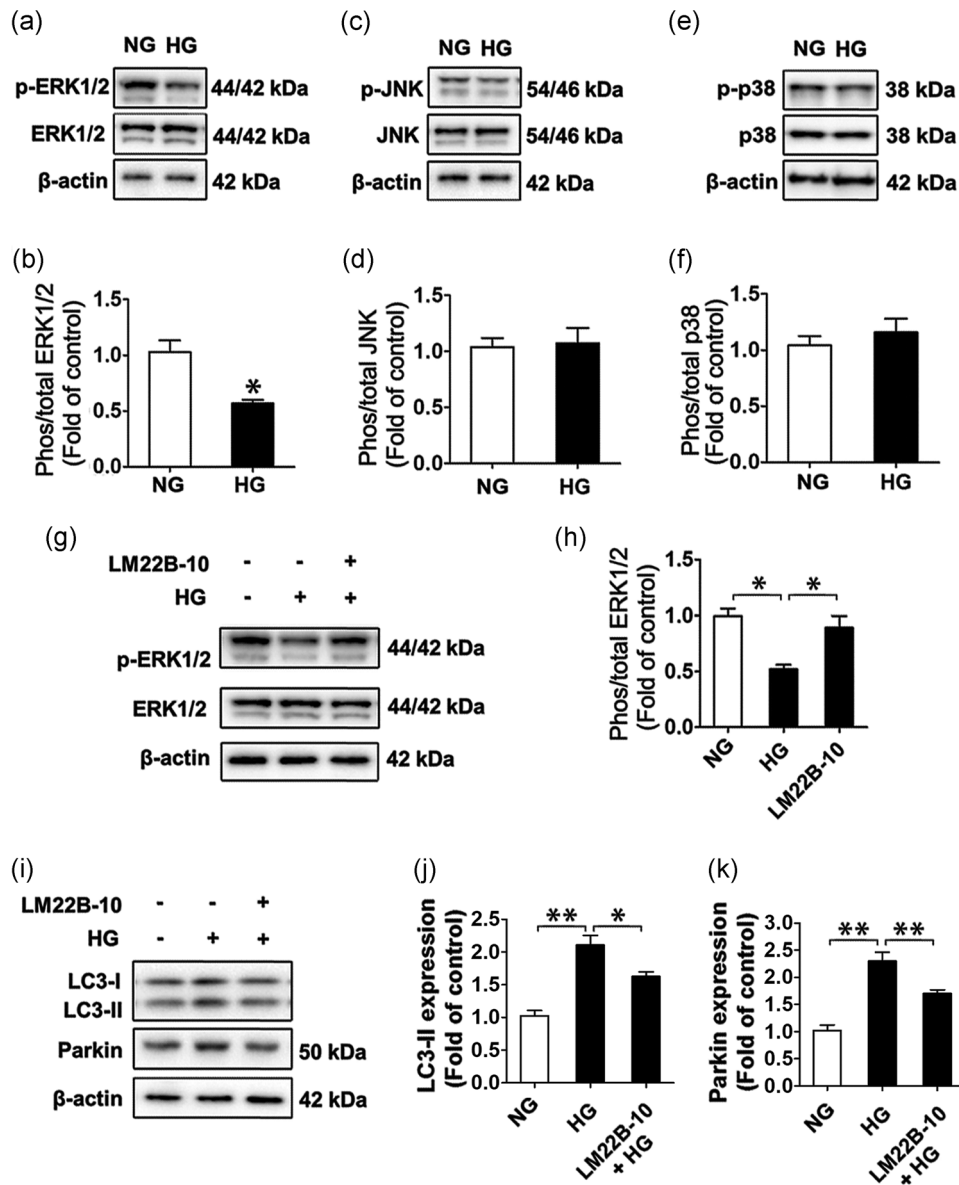


**FIGURE 8** ERK1/2 is required for HG-induced mitophagy in SMG-C6 cells. The levels of phosphorylated and total ERK1/2 (a and b), JNK (c and d) and p38 (e,f) were detected by western blot analysis.  $\beta$ -Actin was used as a loading control.  $n = 6$ ,  $*p < .05$ . (g and h) Western blot identification the effect of ERK1/2 activator LM22B-10 in SMG-C6 cells after HG treatment.  $n = 3$ ;  $*p < .05$ . (i-k) Expressions of LC3 and Parkin were detected by western blot analysis after stimulation with HG, LM22B-10, alone or in combination.  $n = 6$ ;  $*p < .05$ ;  $**p < .01$ . ERK1/2, extracellular regulated protein kinases1/2; HG, high glucose; JNK, c-Jun NH<sub>2</sub>-terminal kinase; LC3, microtubule-associated protein1 lightchain 3; NG, normal glucose; SMG, submandibular gland

#### ACKNOWLEDGEMENTS

The authors thank Dr. David O. Quissell (School of Dentistry, University of Colorado Health Sciences Center, Denver, CO) for the generous gift of rat SMG-C6 cell line. National Natural Science Foundation of China, Grant/Award number: 81570993; Beijing Natural Science Foundation, Grant/Award number: 7162100.

#### CONFLICT OF INTEREST

No potential conflicts of interest relevant to this article were reported.

#### AUTHOR CONTRIBUTIONS

R.-L. X. performed and designed experiments, analyzed, and interpreted data, and wrote the manuscript. Y. H., Y. Z., X. C., and Z.-J. Z. performed the experiments. L.-L. W. and G.-Y. Y. contributed to discussions and reviewed and edited the manuscript.

#### DATA AVAILABILITY

The data that support the findings of this study are available from the corresponding author upon reasonable request.

## ORCID

Ruo-Lan Xiang  <http://orcid.org/0000-0001-5935-1911>

## REFERENCES

- Bajaj, S., Prasad, S., Gupta, A., & Singh, V. B. (2012). Oral manifestations in type-2 diabetes and related complications. *Indian Journal of Endocrinology and Metabolism*, 16(5), 777–779. <https://doi.org/10.4103/2230-8210.100673>.
- Baltrusch, S. (2016). Mitochondrial network regulation and its potential interference with inflammatory signals in pancreatic beta cells. *Diabetologia*, 59(4), 683–687. <https://doi.org/10.1007/s00125-016-3891-x>.
- Bhatti, J. S., Bhatti, G. K., & Reddy, P. H. (2017). Mitochondrial dysfunction and oxidative stress in metabolic disorders - A step towards mitochondria based therapeutic strategies. *Biochimica et Biophysica Acta*, 1863(5), 1066–1077. <https://doi.org/10.1016/j.bbadis.2016.11.010>.
- Blake, R., & Trounce, I. A. (2014). Mitochondrial dysfunction and complications associated with diabetes. *Biochimica et Biophysica Acta*, 1840(4), 1404–1412. <https://doi.org/10.1016/j.bbagen.2013.11.007>.
- Brinkmann, C., Przyklenk, A., Metten, A., Schiffer, T., Bloch, W., Brixius, K., & Gehlert, S. (2017). Influence of endurance training on skeletal muscle mitophagy regulatory proteins in type 2 diabetic men. *Endocrine Research*, 42(4), 325–330. <https://doi.org/10.1080/07435800.2017.1323914>.
- Chen, F., Wen, X., Lin, P., Chen, H., Wang, A., & Jin, Y. (2019). HERP depletion inhibits zearalenone-induced apoptosis through autophagy activation in mouse ovarian granulosa cells. *Toxicology Letters*, 301, 1–10. <https://doi.org/10.1016/j.toxlet.2018.10.026>.
- Chen, L., Liu, C., Gao, J., Xie, Z., Chan, L. W. C., Keating, D. J., ... Yang, S. (2017). Inhibition of Miro1 disturbs mitophagy and pancreatic beta-cell function interfering insulin release via IRS-Akt-Foxo1 in diabetes. *Oncotarget*, 8(53), 90693–90705. <https://doi.org/10.18632/oncotarget.20963>.
- Cong, X., Zhang, Y., He, Q. H., Wei, T., Zhang, X. M., Zhang, J. Z., ... Wu, L. L. (2017). Endothelial tight junctions are opened in cholinergic-evoked salivation in vivo. *Journal of Dental Research*, 96(5), 562–570. <https://doi.org/10.1177/0022034516685048>.
- Devi, T. S., Somayajulu, M., Kowluru, R. A., & Singh, L. P. (2017). TXNIP regulates mitophagy in retinal Muller cells under high-glucose conditions: Implications for diabetic retinopathy. *Cell Death & Disease*, 8(5), e2777. <https://doi.org/10.1038/cddis.2017.190>.
- Feng, J. K., Lu, Y. F., Li, J., Qi, Y. H., Yi, M. L., & Ma, D. Y. (2015). Upregulation of salivary alpha2 macroglobulin in patients with type 2 diabetes mellitus. *Genetics and Molecular Research*, 14(1), 2268–2274. <https://doi.org/10.4238/2015>.
- Hoshino, A., Ariyoshi, M., Okawa, Y., Kaimoto, S., Uchihashi, M., Fukai, K., ... Matoba, S. (2014). Inhibition of p53 preserves Parkin-mediated mitophagy and pancreatic beta-cell function in diabetes. *Proceedings of the National Academy of Sciences U S A*, 111(8), 3116–3121. <https://doi.org/10.1073/pnas.1318951111>.
- Ittichaicharoen, J., Apaijai, N., Tanajak, P., Sa-Nguanmoo, P., Chattipakorn, N., & Chattipakorn, S. C. (2017). Impaired mitochondria and intracellular calcium transients in the salivary glands of obese rats. *Applied Physiology Nutrition and Metabolism*, 42(4), 420–429. <https://doi.org/10.1139/apnm-2016-0545>.
- Jin, G., Xu, C., Zhang, X., Long, J., Rezaeian, A. H., Liu, C., ... Lin, H. K. (2018). Atad3a suppresses Pink1-dependent mitophagy to maintain homeostasis of hematopoietic progenitor cells. *Nature Immunology*, 19(1), 29–40. <https://doi.org/10.1038/s41590-017-0002-1>.
- Jitrapakdee, S., Wutthisathapornchai, A., Wallace, J. C., & MacDonald, M. J. (2010). Regulation of insulin secretion: Role of mitochondrial signalling. *Diabetologia*, 53(6), 1019–1032. <https://doi.org/10.1007/s00125-010-1685-0>.
- Kelley, D. E., He, J., Menshikova, E. V., & Ritov, V. B. (2002). Dysfunction of mitochondria in human skeletal muscle in type 2 diabetes. *Diabetes*, 51(10), 2944–2950. <https://doi.org/10.2337/diabetes.51.10.2944>.
- Larsen, S., Stride, N., Hey-Mogensen, M., Hansen, C. N., Andersen, J. L., Madsbad, S., ... Dela, F. (2011). Increased mitochondrial substrate sensitivity in skeletal muscle of patients with type 2 diabetes. *Diabetologia*, 54(6), 1427–1436. <https://doi.org/10.1007/s00125-011-2098-4>.
- Lilliu, M. A., Solinas, P., Cossu, M., Puxeddu, R., Loy, F., Isola, R., ... Isola, M. (2015). Diabetes causes morphological changes in human submandibular gland: A morphometric study. *Journal of Oral Pathology & Medicine*, 44(4), 291–295. <https://doi.org/10.1111/jop.12238>.
- Lima, D. L. F., Carneiro, S., Barbosa, F. T. S., Saintrain, M. V. L., Moizan, J. A. H., & Doucet, J. (2017). Salivary flow and xerostomia in older patients with type 2 diabetes mellitus. *PLoS One*, 12(8), e0180891. <https://doi.org/10.1371/journal.pone.0180891>.
- Malicka, B., Kaczmarek, U., & Skoskiewicz-Malinowska, K. (2015). Selected antibacterial factors in the saliva of diabetic patients. *Archives of Oral Biology*, 60(3), 425–431. <https://doi.org/10.1016/j.archoralbio.2014.07.010>.
- Masser, D. R., Ojalora, L., Clark, N. W., Kinter, M. T., Elliott, M. H., & Freeman, W. M. (2017). Functional changes in the neural retina occur in the absence of mitochondrial dysfunction in a rodent model of diabetic retinopathy. *Journal of Neurochemistry*, 143(5), 595–608. <https://doi.org/10.1111/jnc.14216>.
- Mathison, R. D., Davison, J. S., Befus, A. D., & Gingerich, D. A. (2010). Salivary gland derived peptides as a new class of anti-inflammatory agents: Review of preclinical pharmacology of C-terminal peptides of SMR1 protein. *Journal of Inflammation (London)*, 7, 49. <https://doi.org/10.1186/1476-9255-7-49>.
- Matsuda, N., Sato, S., Shiba, K., Okatsu, K., Saisho, K., Gautier, C. A., ... Tanaka, K. (2010). PINK1 stabilized by mitochondrial depolarization recruits Parkin to damaged mitochondria and activates latent Parkin for mitophagy. *Journal of Cell Biology*, 189(2), 211–221. <https://doi.org/10.1083/jcb.200910140>.
- Mednieks, M. I., Szczepanski, A., Clark, B., & Hand, A. R. (2009). Protein expression in salivary glands of rats with streptozotocin diabetes. *International Journal of Experimental Pathology*, 90(4), 412–422. <https://doi.org/10.1111/j.1365-2613.2009.00662.x>.
- Morino, K., Petersen, K. F., Sono, S., Choi, C. S., Samuel, V. T., Lin, A., ... Shulman, G. I. (2012). Regulation of mitochondrial biogenesis by lipoprotein lipase in muscle of insulin-resistant offspring of parents with type 2 diabetes. *Diabetes*, 61(4), 877–887. <https://doi.org/10.2337/db11-1391>.
- Nacarelli, T., Azar, A., & Sell, C. (2016). Mitochondrial stress induces cellular senescence in an mTORC1-dependent manner. *Free Radical Biology & Medicine*, 95, 133–154. <https://doi.org/10.1016/j.freeradbiomed.2016.03.008>.
- Park, J. H., Ko, J., Park, Y. S., Park, J., Hwang, J., & Koh, H. C. (2017). Clearance of damaged mitochondria through PINK1 stabilization by JNK and ERK MAPK signaling in chlorpyrifos-treated neuroblastoma cells. *Molecular Neurobiology*, 54(3), 1844–1857. <https://doi.org/10.1007/s12035-016-9753-1>.
- Pipatpi boon, N., Pintana, H., Pratchayasakul, W., Chattipakorn, N., & Chattipakorn, S. C. (2013). DPP4-inhibitor improves neuronal insulin receptor function, brain mitochondrial function and cognitive function in rats with insulin resistance induced by high-fat diet consumption. *The European Journal of Neuroscience*, 37(5), 839–849. <https://doi.org/10.1111/ejn.12088>.
- Ritov, V. B., Menshikova, E. V., Azuma, K., Wood, R., Toledo, F. G., Goodpaster, B. H., ... Kelley, D. E. (2010). Deficiency of electron transport chain in human skeletal muscle mitochondria in type 2 diabetes mellitus and obesity. *American Journal of*

- Physiology-Endocrinology and Metabolism*, 298(1), E49–E58. <https://doi.org/10.1152/ajpendo.00317.2009>.
- Shi, R., Guberman, M., & Kirshenbaum, L. A. (2017). Mitochondrial quality control: The role of mitophagy in aging. *Trends in Cardiovascular Medicine*, 28(4), 246–260. <https://doi.org/10.1016/j.tcm.2017.11.008>.
- Sindhu, S., Akhter, N., Kochumon, S., Thomas, R., Wilson, A., Shenouda, S., ... Ahmad, R. (2018). Increased expression of the innate immune receptor TLR10 in obesity and type-2 diabetes: Association with ROS-mediated oxidative stress. *Cellular Physiology and Biochemistry*, 45(2), 572–590. <https://doi.org/10.1159/000487034>.
- Tickotsky, N., & Ofran, Y. (2017). Integrating genomic data from high-throughput studies with computational modeling reveals differences in the molecular basis of hyposalivation between type 1 and type 2 diabetes. *Clinical Oral Investigations*, 22(1), 151–159. <https://doi.org/10.1007/s00784-017-2094-2>.
- Venegas, V., & Halberg, M. C. (2012). Measurement of mitochondrial DNA copy number. *Methods in Molecular Biology*, 837, 327–335. [https://doi.org/10.1007/978-1-61779-504-6\\_22](https://doi.org/10.1007/978-1-61779-504-6_22).
- Vernon, P. J., & Tang, D. (2013). Eat-me: Autophagy, phagocytosis, and reactive oxygen species signaling. *Antioxidants & Redox Signaling*, 18(6), 677–691. <https://doi.org/10.1089/ars.2012.4810>.
- Volpe, C. M. O., Villar-Delfino, P. H., Dos Anjos, P. M. F., & Nogueira-Machado, J. A. (2018). Cellular death, reactive oxygen species (ROS) and diabetic complications. *Cell Death & Disease*, 9(2), 119. <https://doi.org/10.1038/s41419-017-0135-z>.
- Xiang, R. L., Mei, M., Cong, X., Li, J., Zhang, Y., Ding, C., ... Yu, G. Y. (2014). Claudin-4 is required for AMPK-modulated paracellular permeability in submandibular gland cells. *Journal of Molecular Cell Biology*, 6(6), 486–497. <https://doi.org/10.1093/jmcb/mju048>.
- Xiao, B., Deng, X., Lim, G. G. Y., Xie, S., Zhou, Z. D., Lim, K. L., & Tan, E. K. (2017). Superoxide drives progression of Parkin/PINK1-dependent mitophagy following translocation of Parkin to mitochondria. *Cell Death & Disease*, 8(10), e3097. <https://doi.org/10.1038/cddis.2017.463>.
- Yu, T., Robotham, J. L., & Yoon, Y. (2006). Increased production of reactive oxygen species in hyperglycemic conditions requires dynamic change of mitochondrial morphology. *Proceedings of the National Academy of Sciences U S A*, 103(8), 2653–2658. <https://doi.org/10.1073/pnas.0511154103>.
- Zalewska, A., Knas, M., Niczyporuk, M., Razak, H. H., Waszkiewicz, N., Przystupa, A. W., ... Zarzycki, W. (2013). Salivary lysosomal exoglycosidases profiles in patients with insulin-dependent and noninsulin-dependent diabetes mellitus. *Advances in Clinical and Experimental Medicine*, 22(5), 659–666.
- Zhang, C. L., Feng, H., Li, L., Wang, J. Y., Wu, D., Hao, Y. T., ... Wu, L. L. (2017). Globular CTRP3 promotes mitochondrial biogenesis in cardiomyocytes through AMPK/PGC-1alpha pathway. *Biochimica et Biophysica Acta*, 1861(1 Pt A), 3085–3094. <https://doi.org/10.1016/j.bbagen.2016.10.022>.

**How to cite this article:** Xiang R-L, Huang Y, Zhang Y, et al. Type 2 diabetes-induced hyposalivation of the submandibular gland through PINK1/Parkin-mediated mitophagy. *J Cell Physiol*. 2020;235:232–244. <https://doi.org/10.1002/jcp.28962>